Supporting Information

Luminescent Porous Organic Polymer Nanotubes for highly selective sensing of H_2S

Lin Guo[1,‡], Meng Wang,[1,‡] Xiaofei Zeng* and Dapeng Cao[1,2,*]

[1] State Key Laboratory of Organic-Inorganic Composites, Beijing University of Chemical Technology, Beijing 100029, People's Republic of China

[2] Beijing Advanced Innovation Center for Soft Matter Science and Engineering, Beijing University of Chemical Technology, Beijing 100029, People's Republic of China

Table of Contents

S1 Experiments for making COP test paper and sensing detection

In order to facilitate the detection, we assembled COPs into luminescent test paper, the detailed preparation methods are as follow: the blank neutral filter paper dipped into COP suspensions for a few minutes, then took out and dried for subsequent use. To explore the luminescent sensing properties of the COPs test paper for detecting anions, different anion solutions were dripped onto the test paper, and the changes of the luminescent test paper was observed under an UV lamp, where the excitation wavelength λex=365 nm. In order to achieve the detection of gaseous H_2S, the newly prepared moist luminescent test paper was exposed to H_2S atmosphere, and then observed the changes of the luminescent test paper under an UV lamp. To further explore the selectivity of the luminescent test paper for sensing H_2S gas, the changes of the luminescent test paper in different gases was observed under the UV lamp (λex=365 nm).

S2 Experiments for luminescent sensing in vitro assay

PBS buffer solution: Firstly, put KH_2PO_4 (1.701g) to a 500ml volumetric flask, and dissolved by distilled water and diluted to half the volumetric flask. Then, used sodium hydroxide and hydrochloric acid aqueous solution to adjust the buffer solution until PH=7.4. Finally, the PBS buffer solution obtained.

The analytes used for the luminescent sensing experiments are Na_2S, NaF, Na_2SO_4, NaCl, NaBr, NaI, $NaIO_3$, NaSCN, $NaHSO_3$, Na_3PO_4, $NaNO_3$, Na_2CO_3, Cys and Vc, and dissolved in distilled water. The dried powder of PNT-1 dispersed in ethanol aqueous solution (1mg/ml) was ultra-sonicated for an hour, and obtained the PNT-1-EtOH suspension for the following experiment. Then, put 0.5 ml PNT-1-EtOH suspension to 4.5

ml PBS buffer solution, ultrasonic until uniformity mixtured. The photoluminescence (PL) sensing properties of the synthesized PNT-1 material in PBS buffer solution were investigated at room temperature. To explore the luminescent properties of the PNT-1 for sensing these analytes, the fluorescence spectra of PNT-1 suspension were recorded by successive addition of aliquots of analytes (S^{2-}, F^-, SO_4^{2-}, Cl^-, Br^-, I^-, IO_3^-, SCN^-, HSO_3^-, PO_4^{3-}, NO_3^-, CO_3^{2-}, Cys and Vc, respectively). The widths of the excitation slit are 5 nm and emission slit is 10 nm for PNT-1.

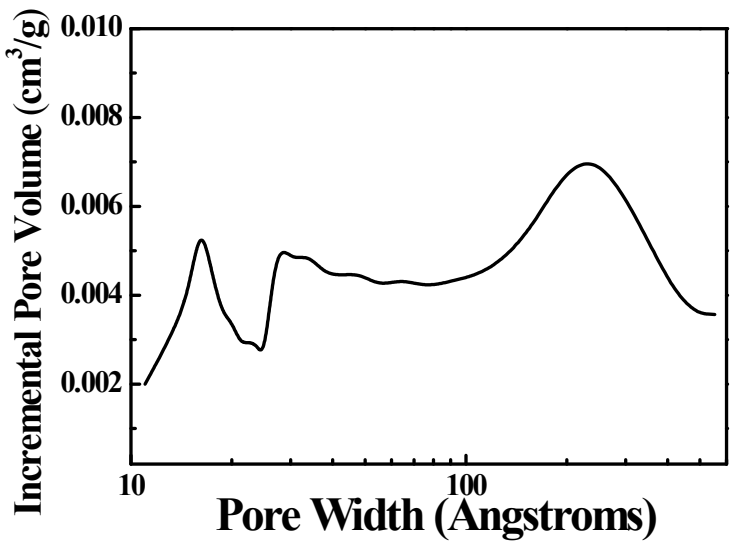

Figure S1. Nonlocal density functional theory (NLDFT) pore size distributions of PNT-1 by incremental pore volume.

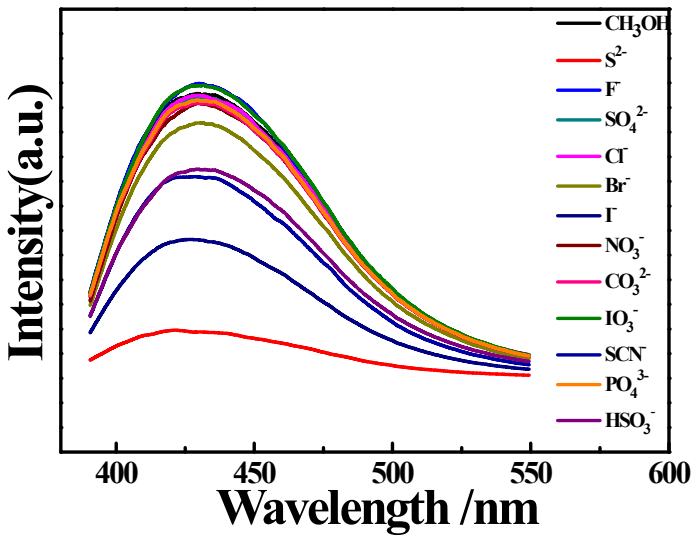

Figure S2 Fluorescence spectra of PNT-1 dispersed in CH_3OH solutions after adding different anions.

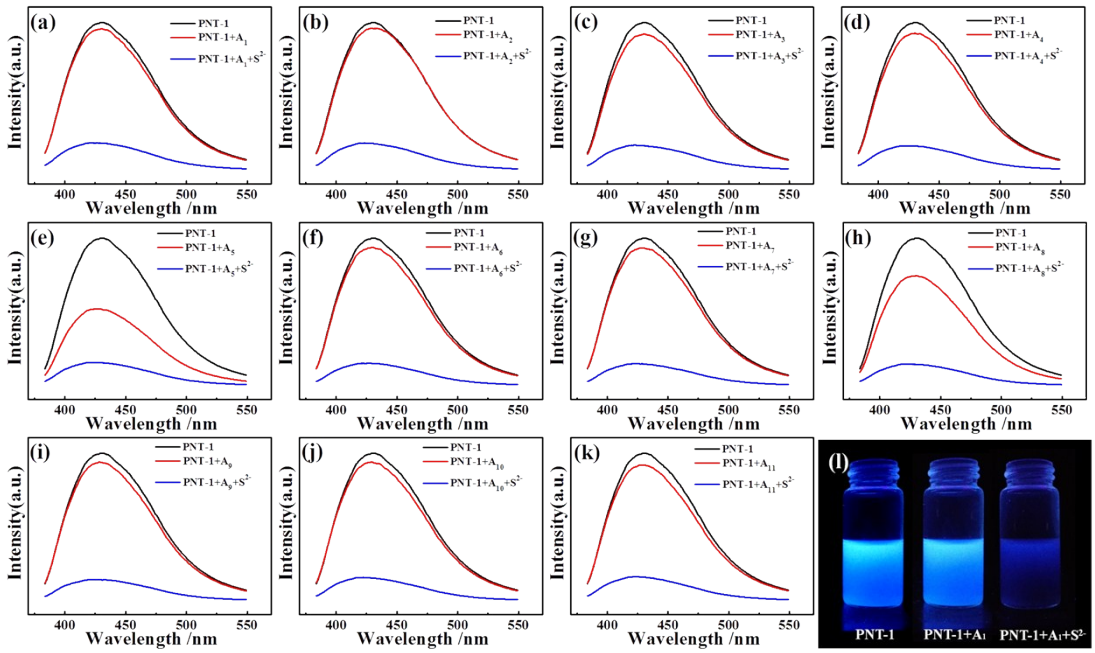

Figure S3 (a)~(k): The luminescence emission spectra of PNT-1 before (black line) and after adding A_x (red line) and A_x+S^{2-} (blue line) in methanol solution, (x=1~11, A_1: F^-; A_2: SO_4^{2-}; A_3: Cl^-; A_4: Br^-; A_5: I^-; A_6: NO_3^- ; A_7: CO_3^{2-}; A_8: IO_3^-; A_9: SCN^- ; A_{10}: PO_4^{3-}; A_{11}: HSO_3^-), where the widths of the excitation slit are 5 nm and emission slit is 10 nm for PNT-1. (l) The luminescence intensity of PNT-1 before and after adding A_x and A_x' in methanol solution, $A_x'=A_x+S^{2-}$.(g) the PL quenching photograph by before and after adding anions into PNT-1 suspensions in methanol solutions, where PL is excited under λex=365 nm using a portable UV lamp.

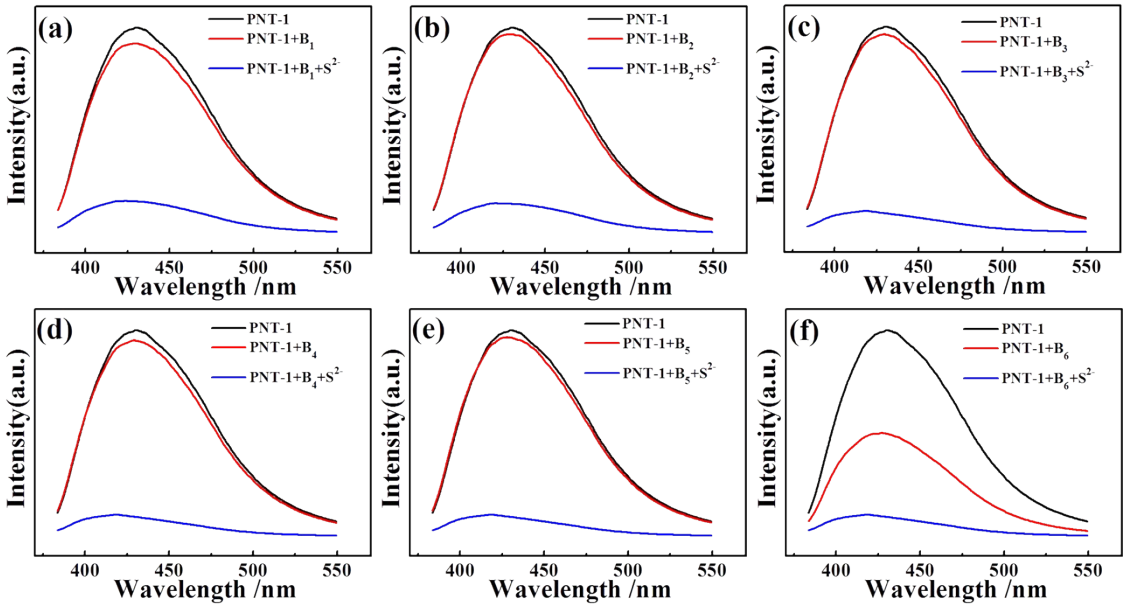

Figure S4 (a)~(f): The luminescence emission spectra of PNT-1 before (black line) and after adding B_x (red line) and B_x+S^{2-} (blue line) in methanol solution, (x=1~6, **B_1:** SO_4^{2-}+F^-; **B_2:** Cl^-+F^-; **B_3:** SO_4^{2-}+NO_3^- ; **B_4:** IO_3^-+NO_3^- ; **B_5:** Br^-+HSO_3^-; **B_6:** Cl^-+I^-), where the widths of the excitation slit are 5 nm and emission slit is 10 nm for PNT-1.

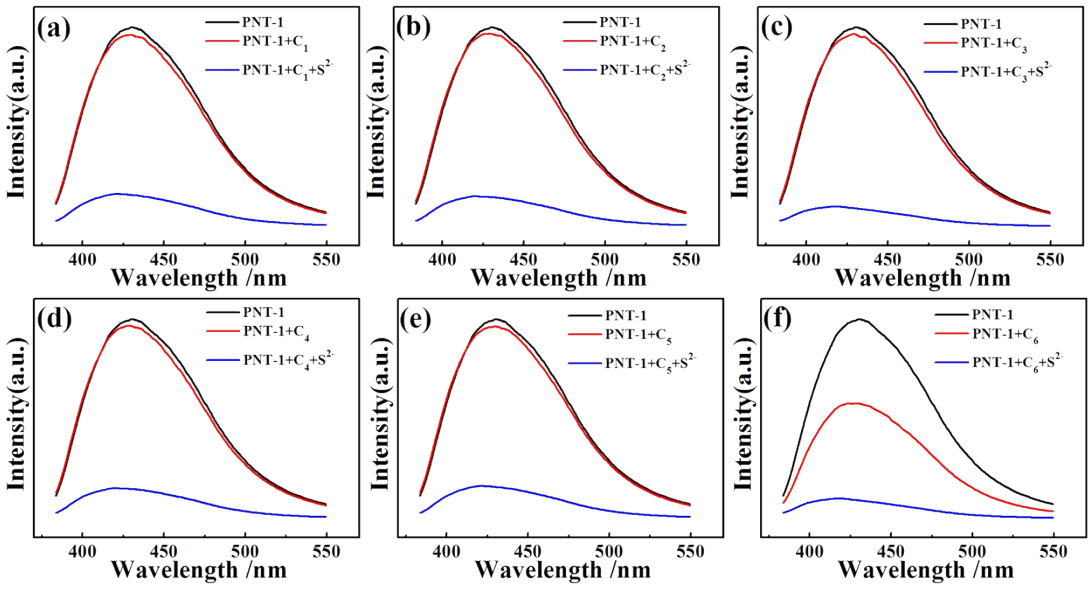

Figure S5 (a)~(f): The luminescence emission spectra of PNT-1 before (black line) and after adding C_x (red line) and C_x+S^{2-} (blue line) in methanol solution, (x=1~6, C_1: SO_4^{2-}+Cl^-+F^-; C_2: Cl^-+F^-+HSO_3^-; C_3: SO_4^{2-}+Br^-+NO_3^-; C_4: IO_3^-+Cl^-+NO_3^-; C_5: IO_3^-+Br^-+HSO_3^-; C_6: Cl^-+I^-+SCN^-), where the widths of the excitation slit are 5 nm and emission slit is 10 nm for PNT-1.

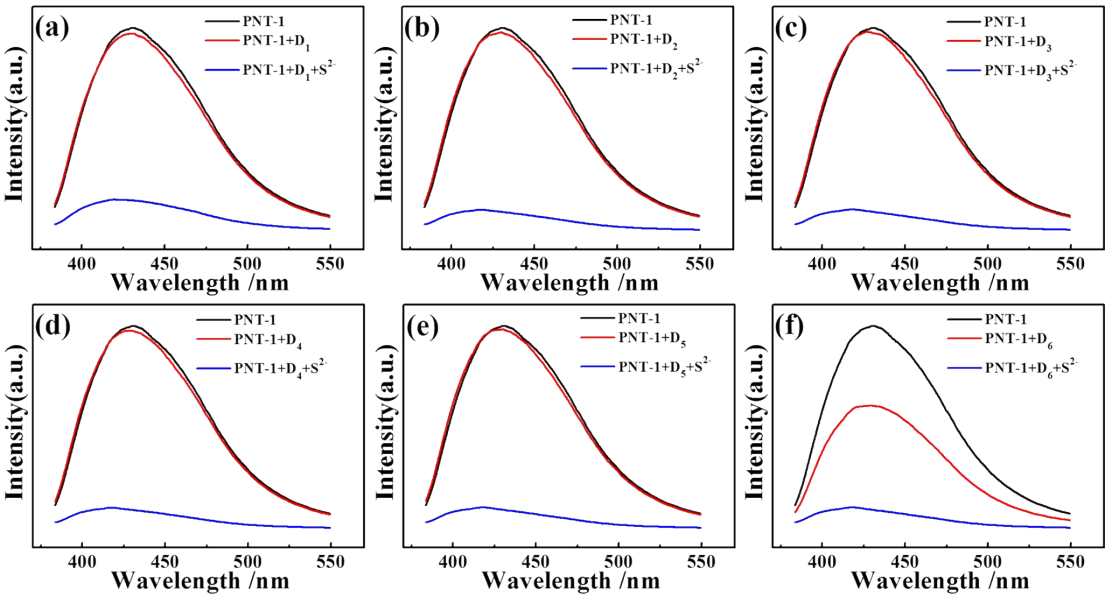

Figure S6 (a)~(f): The luminescence emission spectra of PNT-1 before (black line) and after adding D_x (red line) and D_x+S^{2-} (blue line) in methanol solution, (x=1~6, D_1: SO_4^{2-}+Cl^-+F^-+Br^-; D_2: Cl^-+F^-+HSO_3^-+NO_3^-; D_3: SO_4^{2-}+IO_3^-+Br^-+NO_3^- ; D_4: IO_3^-+Cl^-+Br^-+NO_3^-; D_5: IO_3^-+F^-+Br^-+ HSO_3^-; D_6: Cl^-+HSO_3^-+I^-+SCN^-), where the widths of the excitation slit are 5 nm and emission slit is 10 nm for PNT-1.

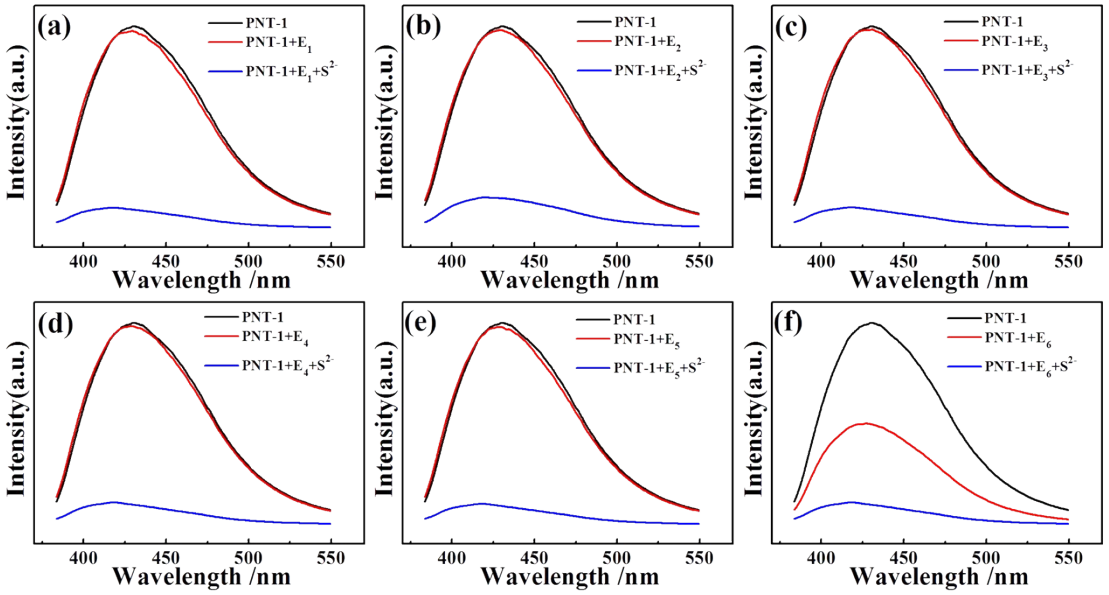

Figure S7 (a)~(f): The luminescence emission spectra of PNT-1 before (black line) and after adding E_x (red line) and E_x+S^{2-} (blue line) in methanol solution, (x=1~6, E_1: SO_4^{2-}+Cl^-+F^-+Br^-+NO_3^- ; E_2: SO_4^{2-}+Cl^-+F^-+HSO_3^-+NO_3^-; E_3: SO_4^{2-}+IO_3^-+Br^-+HSO_3^-+NO_3^-; E_4: IO_3^-+Cl^-+Br^-+HSO_3^-+NO_3^- ; E_5: IO_3^-+F^-+Br^-+HSO_3^-+NO_3^- ; E_6: Cl^-+PO_4^{3-}+HSO_3^-+I^-+SCN^-), where the widths of the excitation slit are 5 nm and emission slit is 10 nm for PNT-1.

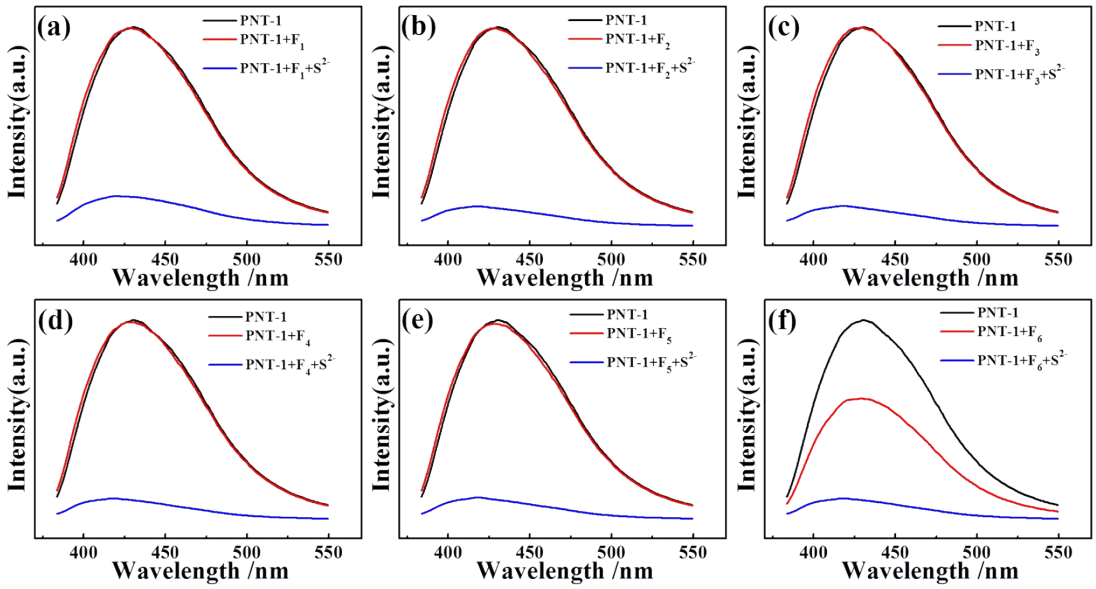

Figure S8 (a)~(f): The luminescence emission spectra of PNT-1 before (black line) and after adding F_x (red line) and F_x+S^{2-} (blue line) in methanol solution, (x=1~6, F_1: SO_4^{2-}+Cl^-+F^-+Br^-+HSO_3^-+NO_3^-; F_2: SO_4^{2-}+IO_3^-+Cl^-+F^-+HSO_3^-+NO_3^-; F_3: SO_4^{2-}+IO_3^-+CO_3^{2-}+Br^-+ HSO_3^-+NO_3^-; F_4: IO_3^-+CO_3^{2-}+Cl^-+Br^-+HSO_3^- +NO_3^-; F_5: IO_3^-+CO_3^{2-}+F^-+Br^-+HSO_3^-+NO_3^-; F_6:Cl^-+ PO_4^{3-}+Br^-+HSO_3^-+I^-+SCN^-), where the widths of the excitation slit are 5 nm and emission slit is 10 nm for PNT-1.

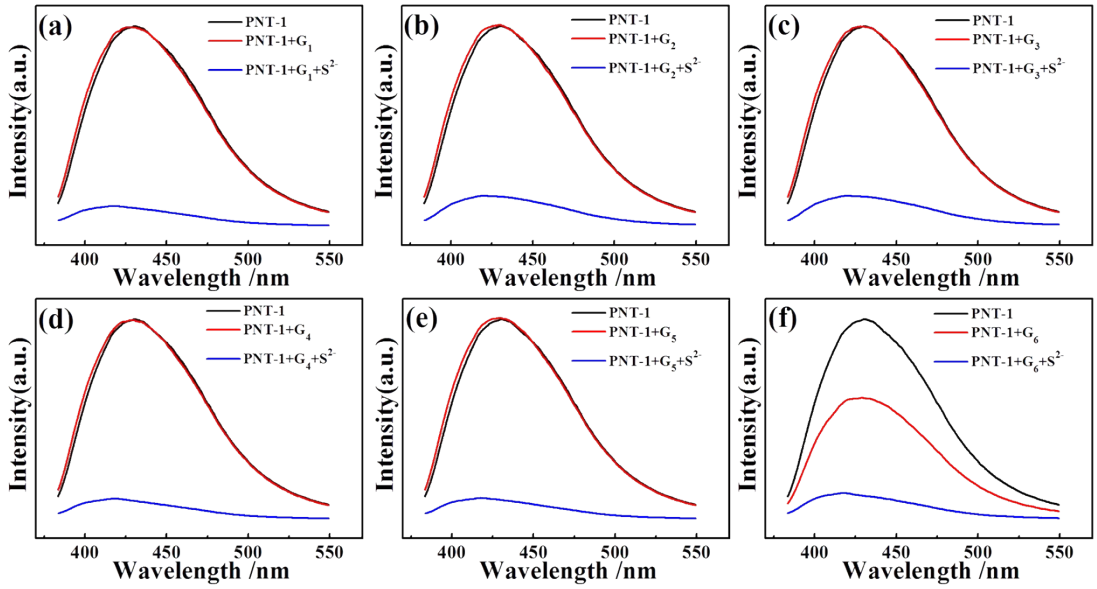

Figure S9 (a)~(f): The luminescence emission spectra of PNT-1 before (black line) and after adding G_x (red line) and G_x+S^{2-} (blue line) in methanol solution, (x=1~6, G_1: SO_4^{2-}+CO_3^{2-}+Cl^-+F^-+Br^-+HSO_3^-+NO_3^-; G_2: SO_4^{2-}+IO_3^-+CO_3^{2-}+Cl^-+F^-+HSO_3^-+NO_3^-; G_3: SO_4^{2-}+ IO_3^-+CO_3^{2-}+PO_4^{3-}+Br^-+HSO_3^-+NO_3^-; G_4: IO_3^-+CO_3^{2-}+Cl^-+PO_4^{3-}+Br^-+HSO_3^-+NO_3^-; G_5: IO_3^-+ CO_3^{2-}+F^-+PO_4^{3-}+Br^-+HSO_3^-+NO_3^-; G_6:SO_4^{2-}+Cl^-+PO_4^{3-}+ Br^-+HSO_3^-+I^-+SCN^-), where the widths of the excitation slit are 5 nm and emission slit is 10 nm for PNT-1.

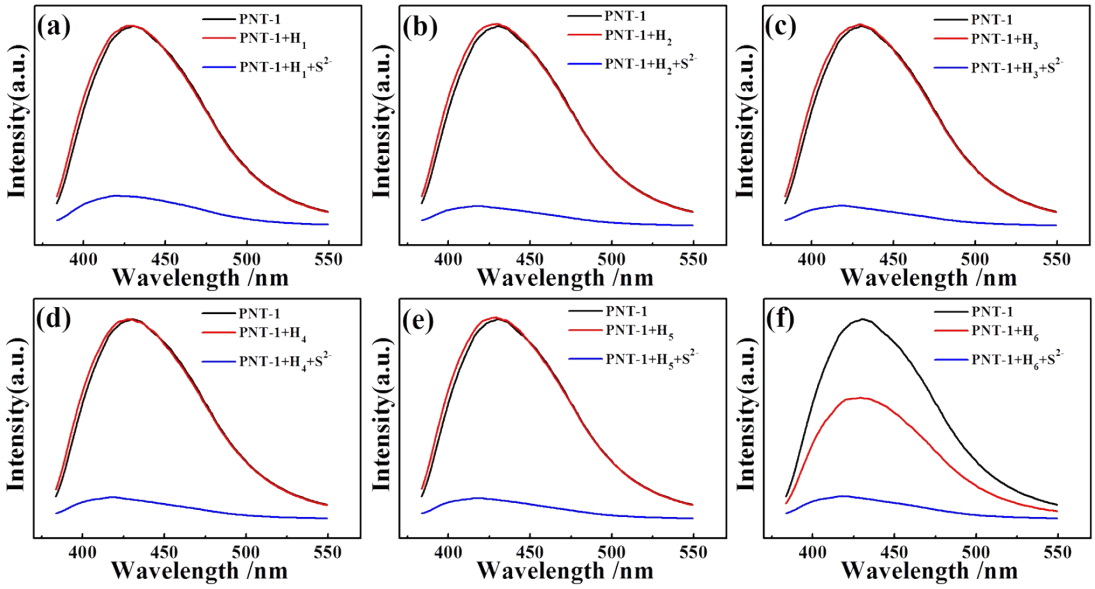

Figure S10 (a)~(f): The luminescence emission spectra of PNT-1 before (black line) and after adding H_x (red line) and H_x+S^{2-} (blue line) in methanol solution, (x=1~6, H_1: $SO_4^{2-}+IO_3^-+CO_3^{2-}+Cl^-+F^-+PO_4^{3-}+Br^-+NO_3^-$; H_2: $SO_4^{2-}+IO_3^-+CO_3^{2-}+Cl^-+F^-+Br^-+HSO_3^-+NO_3^-$; H_3: $SO_4^{2-}+IO_3^-+CO_3^{2-}+Cl^-+PO_4^{3-}+Br^-+HSO_3^-+NO_3^-$; H_4: $SO_4^{2-}+IO_3^-+CO_3^{2-}+F^-+PO_4^{3-}+Br^-+HSO_3^-+NO_3^-$; H_5: $SO_4^{2-}+IO_3^-+CO_3^{2-}+Cl^-+F^-+PO_4^{3-}+HSO_3^-+NO_3^-$; H_6: $SO_4^{2-}+IO_3^-+CO_3^{2-}+Cl^-+F^-+PO_4^{3-}+Br^-+HSO_3^-+NO_3^-+I^-+SCN^-$), where the widths of the excitation slit are 5 nm and emission slit is 10 nm for PNT-1.

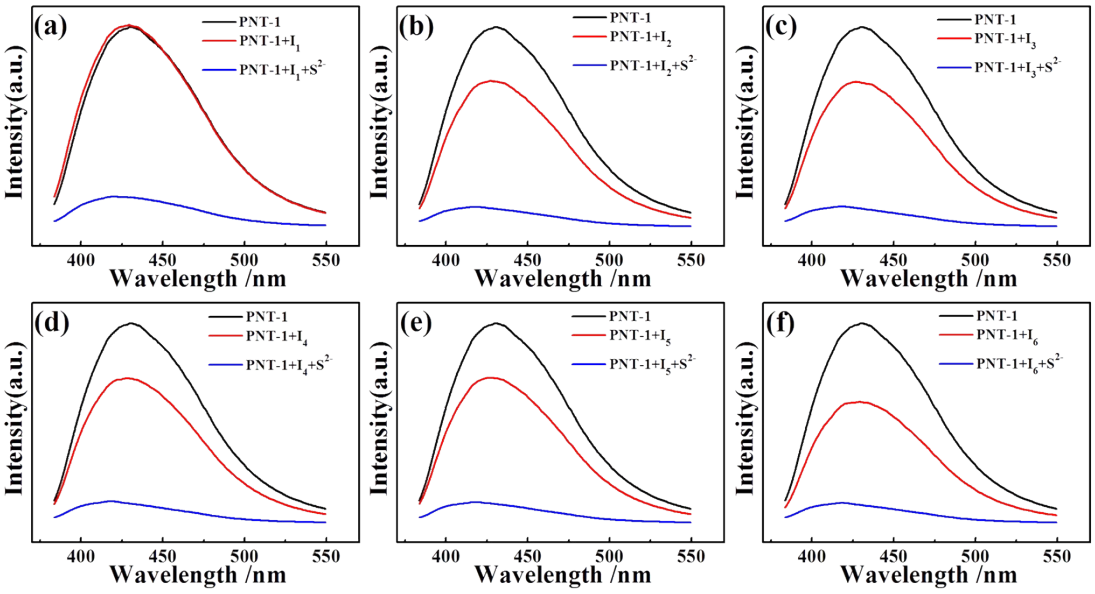

Figure S11 (a)~(f): The luminescence emission spectra of PNT-1 before (black line) and after adding I_x (red line) and I_x+S^{2-} (blue line) in methanol solution, (x=1~6, I_1: $SO_4^{2-}+IO_3^-+CO_3^{2-}+F^-+Cl^-+PO_4^{3-}+Br^-+HSO_3^-+NO_3^-$; I_2: $SO_4^{2-}+IO_3^-+CO_3^{2-}+F^-+Cl^-+Br^-+HSO_3^-+NO_3^-+SCN^-$; I_3: $SO_4^{2-}+IO_3^-+CO_3^{2-}+F^-+PO_4^{3-}+Br^-+HSO_3^-+NO_3^-+SCN^-$; I_4: $SO_4^{2-}+IO_3^-+CO_3^{2-}+Cl^-+PO_4^{3-}+Br^-+HSO_3^-+NO_3^-+SCN^-$; I_5: $SO_4^{2-}+IO_3^-+F^-+Cl^-+PO_4^{3-}+Br^-+HSO_3^-+NO_3^-+SCN^-$; I_6: $SO_4^{2-}+IO_3^-+CO_3^{2-}+Cl^-+PO_4^{3-}+Br^-+HSO_3^-+I^-+SCN^-$), where the widths of the excitation slit are 5 nm and emission slit is 10 nm for PNT-1.

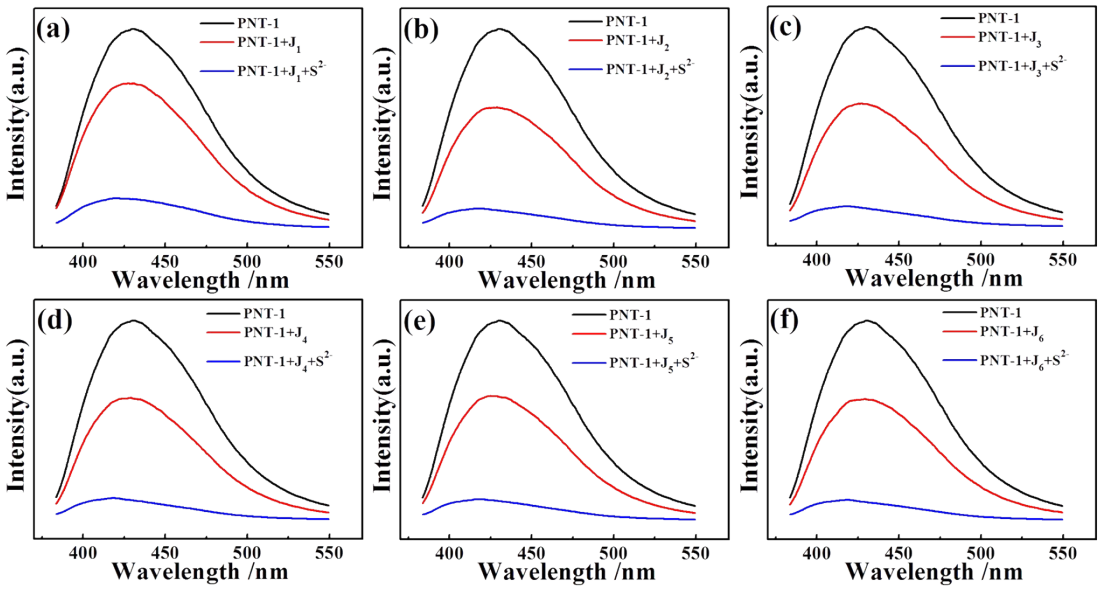

Figure S12 (a)~(f): The luminescence emission spectra of PNT-1 before (black line) and after adding J_x (red line) and J_x+S^{2-} (blue line) in methanol solution, (x=1~6, J_1: $SO_4^{2-}+IO_3^-+CO_3^{2-}+F^-+Cl^-+PO_4^{3-}+Br^-+HSO_3^-+NO_3^-+SCN^-$; J_2: $SO_4^{2-}+IO_3^-+CO_3^{2-}+F^-+Cl^-+PO_4^{3-}+Br^-+HSO_3^-+I^-+SCN^-$; J_3: $SO_4^{2-}+IO_3^-+CO_3^{2-}+Cl^-+PO_4^{3-}+Br^-+HSO_3^-+NO_3^-+I^-+SCN^-$; J_4: $SO_4^{2-}+IO_3^-+CO_3^{2-}+F^-+PO_4^{3-}+Br^-+HSO_3^-+NO_3^-+I^-+SCN^-$;$J_5$: $IO_3^-+CO_3^{2-}+F^-+Cl^-+PO_4^{3-}+Br^-+HSO_3^-+NO_3^-+I^-+SCN^-$; J_6: $SO_4^{2-}+IO_3^-+CO_3^{2-}+Cl^-+PO_4^{3-}+Br^-+HSO_3^-+NO_3^-+I^-+SCN^-$), where the widths of the excitation slit are 5 nm and emission slit is 10 nm for PNT-1.

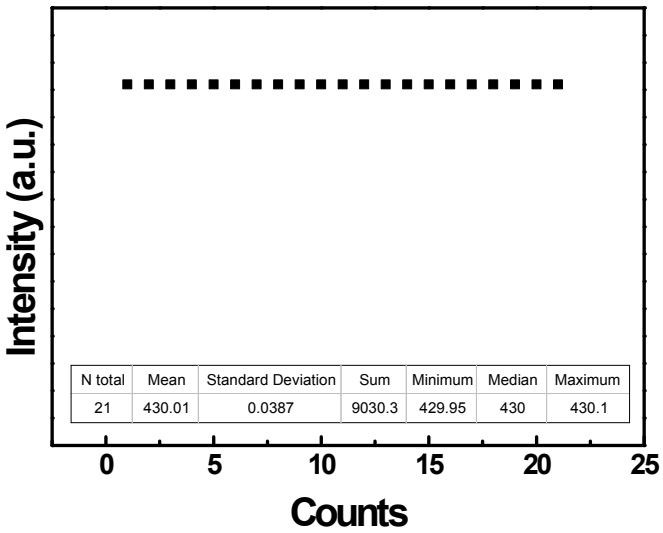

N total	Mean	Standard Deviation	Sum	Minimum	Median	Maximum
21	430.01	0.0387	9030.3	429.95	430	430.1

Figure S13. Luminescent intensity of PNT-1 dispersed in methanol solution after different measurements.

The limited of detection concentration of PNT-1 for sensing analytes can be calculated by the equation of LOD=3σ/k, where σ is standard deviation of the blank luminescent materials, k is the k_{sv} constant of the materials for sensing analytes.

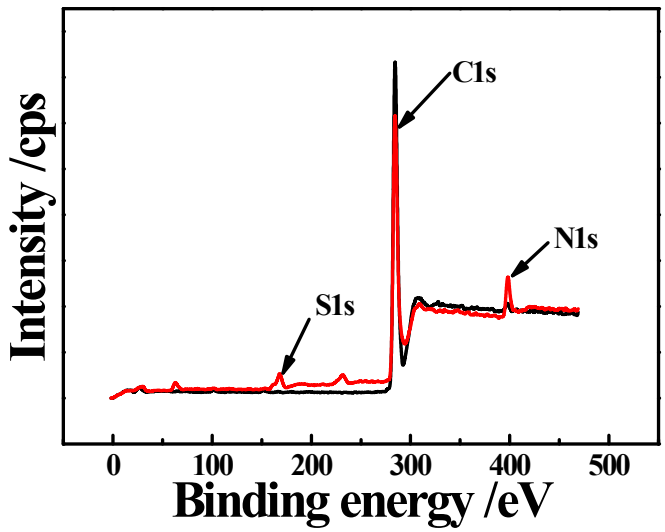

Figure S14 XPS spectra of PNT-1 (black line) and PNT-1a (red line) .

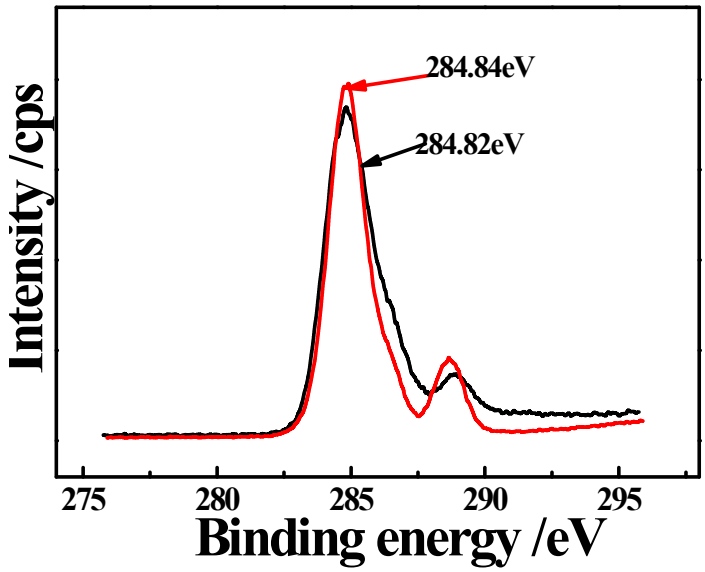

Figure S15 High-resolution C1s XPS spectra of (a) PNT-1 and (b) PNT-1a.

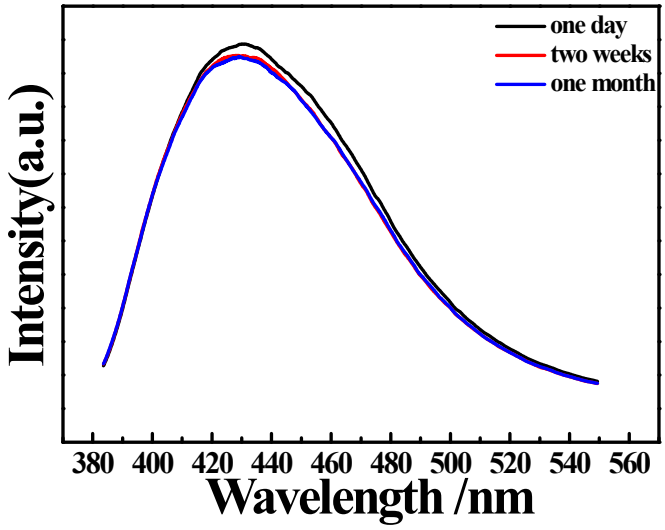

Figure S16 PL spectra of PNT-1 dispersed in CH_3OH solutions in different placement times.

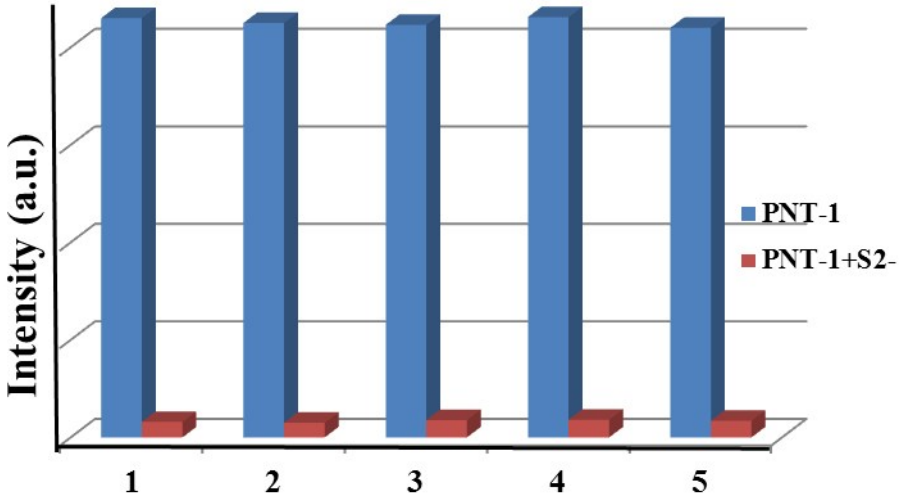

Figure S17 The luminescence intensity of PNT-1 for sensing S^{2-} in five recycles.

Table S1 Comparison of luminescent probe for sensing H_2S gas.

Probe	λex/λem (nm)	Detection limit (mol/L)	Ref
Eu^{3+}/Cu^{2+}@UiO-66-$(COOH)_2$	393/615	5.45×10^{-6}	1
Fe^{III}-MIL-88-NH_2	333/440	10×10^{-6}	2
mesoporous silica nanoparticles	405/590	2.7×10^{-6}	3
$Zn(L)(4,4'\text{-bpy})_{0.5}].(H_2O)_{0.25}$	466/560	7.9×10^{-6}	4
Europium(III) based probe	350/580	9.6×10^{-6}	5
Sensors derived from azide or nitro	480/525	10×10^{-6}	6
Azamacrocyclic Cu(II) ion complex	479/535	10×10^{-6}	7
TPM	352/529	10×10^{-6}	8
This work	370/425	1.8×10^{-6}	

References

1. X. Zhang, Q. Hu, T. Xia, et al. ACS appl. Mater. Inter., 2016, 8(47): 32259-32265.
2. Y. Cao, X. F. Guo, H. Wang. Sensor. Actuat. B-Chem., 2017, 243: 8-13.
3. Q. Yu, K. Y. Zhang, H. Liang, et al. ACS appl. Mater. Inter., 2015, 7(9): 5462-5470.
4. X. F. Yang, H. B. Zhu, M. Liu. Inorganica Chimica Acta, 2017, 466: 410-416.
5. Y. W. Yip, G. L. Law, W. T. Wong. Dalton T., 2016, 45(3): 928-935.
6. A. R. Lippert, E. J. New, C. J. Chang. J. Am. Chem. Soc., 2011, 133(26): 10078-10080.
7. K. Sasakura, K. Hanaoka, N. Shibuya, et al. J. Am. Chem. Soc., 2011, 133(45): 18003-18005.
8. S. K. Das, C. S. Lim, S. Y. Yang, et al. Chem. Commun., 2012, 48(67): 8395-8397.